Materials Science Forum Vols. 495-497 (2005) pp. 255-260
online at http://www.scientific.net

Combined synchrotron and neutron structural refinement of R-phase in $Ti_{50.75}.Ni_{47.75}.Fe_{1.50}$ shape memory alloy

H. Sitepu[1], J.P. Wright[2], T. Hansen[3], D. Chateigner[4], H.-G. Brokmeier[5], C. Ritter[3], and T. Ohba[6]

[1]Department of Geosciences, Virginia Tech, Blacksburg, VA 24061, USA < sitepu@vt.edu>

[2]European Synchrotron Research Facility (ESRF), BP 220, 38043 Grenoble Cedex, France

[3]Institut Laue-Langevin (ILL) Neutrons for Science, BP 156, 38042 Grenoble Cedex 7, France

[4]CRISMAT-ISMRA, UMR CNRS n° 6508, Bd. Maréchal Juin, 14050 Caen, France

[5]GKSS-Research Center, Max-Planck-Str, D-21502 Geesthacht, Germany

[6]Department of Materials Science, Shimane University, Nishikawatsu, Matsue 690-8504, Japan

Keywords: Synchrotron and neutron powder diffraction; R-phase in Ti-Ni-Fe ternary alloy; Rietveld refinement; Generalized spherical harmonic; Phase composition analysis

Abstract

The crystal structure of R-phase in $Ti_{50.75}.Ni_{47.75}.Fe_{1.50}$ shape memory alloy (SMA) has been studied at a temperature of (290 ± 7) K on cooling by combined synchrotron and neutron powder diffraction using Rietveld refinement with generalized spherical harmonic (GSH) description for preferred orientation (PO). The results showed that (i) no significant improvement in the crystallographic R_{WP}-factor was found when the inversion center was removed from the $P\bar{3}$ model, suggesting that the space group was indeed $P\bar{3}$ and not lower symmetry $P3$ neither $P31m$ and (ii) the refined atomic parameters were converging only when the $P\bar{3}$ space group was used in the refinement.

Introduction

Shape memory effect or superelasticity in $Ti_{50.75}.Ni_{47.75}.Fe_{1.50}$ [1,2 and references therein] and the aged (400°C, 24h) Ni-rich $Ti_{49.3}.Ni_{50.7}$ [3] alloys is based on martensitic phase transformations from *high-temperature* cubic (B2) austenite phase to a monoclinic (B19′) martensite at *low-temperature*, with the trigonal R-phase occurring in an intermediate temperature range. The R-phase transformation is of particular interest because of the curious transformation behaviour and actuators applications due to a very small temperature hysteresis (*e.g.* 1-2K). It is noted, that small additions of Fe into NiTi alloy separate the temperature ranges for B2→R-phase and B2→B19′ transformations by more than 100K [1,2].

In order to understand the mechanism of the transformation, it is necessary to know the crystal structures of the R-phase. The space group of R-phase was initially determined by Goo and Sinclair [4] as $P\bar{3}1m$ (No. 162) using convergent beam electron diffraction (CBED). However, they did not determine the crystal structures. Then, Hara *et al.* [1,2] described the crystal structure of R-phase in the textured rod shaped $Ti_{50.75}{\cdot}Ni_{47.75}{\cdot}Fe_{1.50}$ ternary alloy (10 mm in diameter) by combined use of X-ray powder diffraction (XRD) and electron diffraction method. They showed that (i) the space group of the R-phase is of lower symmetry $P3$ (No. 143) which is the same as that of ζ' Au-Cd alloy, but the deviations of the atom positions from $P\bar{3}1m$ is about half of those of ζ' martensite and (ii) the CBED patterns taken to confirm the $P3$ still supported the $P\bar{3}1m$ space group. However, the precision of the results derived from Rietveld refinements for various XRD data sets of the R-phase needs further special attention because (i) the alloy investigated has fiber texture

[1,2] which had not been corrected and (ii) the weight percentage of the non-transformed austenite had not been determined either. Subsequently, Schryvers and Potapov [5] described the crystal structure of the same alloy but only a small probe size of about 0.05μm in diameter using transmission electron microscope and showed that the atoms in the R-phase structure are located in centrosymetric positions leading to $P\bar{3}$ (No. 147) space group instead of the lower symmetry $P3$. The crystal structure of the textured $Ti_{50.75}$·$Ni_{47.75}$·$Fe_{1.50}$ ternary alloy (see Fig. 1) was non-destructively determined using the third generation synchrotron X-ray sources at ESRF Grenoble, which make available X-ray beams of higher energy and much higher intensity than laboratory X-ray sources for measuring the synchrotron powder diffraction (SRD) data of R-phase during thermal cycling [6,7]. The results obtained from Rietveld refinement with the GSH description for PO correction [8 and references therein] indicated that: (i) for texture in R-phase the reasonable crystal structure parameters was obtained when applying correction to intensities using the GSH description, (ii) the weight percentage of the non-transformed austenite was approximately 3%, and (iii) no significant improvement in goodness-of-fit index was found when the inversion center was removed from the $P\bar{3}$ model, suggesting that the space group was indeed $P\bar{3}$ and not $P3$ [6,7].

The structural refinement and phase composition analysis SRD study of the $P\bar{3}$ model of R-phase in textured $Ti_{50.75}$·$Ni_{47.75}$·$Fe_{1.50}$ ternary alloy has now been extended to neutron diffraction (ND) data. There are two special features of ND in this study. Firstly, ability to measure data to high values of $\sin\theta/\lambda$, which gives better atomic position and/or thermal parameters than X-rays in the resultant crystal structure. This arises from the physics of ND, which ensures that the intensity of the scattering of the neutron beam from individual atoms does not decrease with $\sin\theta/\lambda$ as it does for X-ray scattering. Secondly, ND offers an easier technological route to the development of *in-situ* measurements than for other experimental techniques, mostly because neutrons are not readily absorbed or attenuated by sample environment equipment (*e.g.* cryofurnace). Therefore, ND data might be expected to provide details of the bulk crystal structure and preferred orientation induced by temperature. In the present study, a combined SRD and ND data structural refinement was conducted to clarify the space group of the R-phase. To the best of our knowledge there has been no detailed analysis published in the literature providing information on the combined structural refinement of R-phase using SRD and ND data along with the texture information.

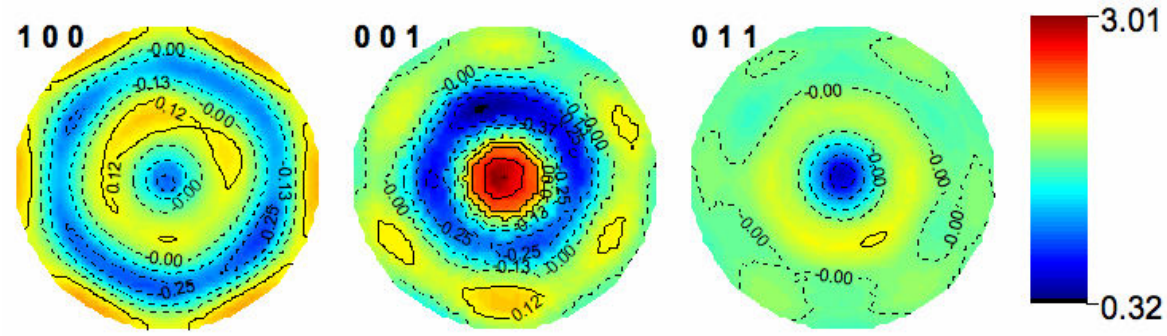

Fig. 1. The first three reflection pole-figures for the R-phase in $Ti_{50.75}$·$Ni_{47.75}$·$Fe_{1.50}$ alloy are given in equal area projection and linear scale. The pole-density scale is shown on the right-hand side and given in multiples of a random distribution. The the WIMV method [9] was used to extract the texture information from a simultaneous refinement with 1368 ND patterns held in a variety of orientations in the ILL D20 texture goniometer. The ODF derived from MAUD and those results obtained from pole-figures measurements conducted at GKSS Geesthacht will be given elsewhere. Note that, MAUD uses the WIMV method to determine the ODF of the sample by assuming some properties [9] of what is in essence the odd orders of the GSH that are not determined by a diffraction experiment. GSAS only determines the even harmonic terms and one must use some other method for getting the rest of the ODF.

Experimental

The textured $Ti_{50.75}$·$Ni_{47.75}$·$Fe_{1.50}$ ternary alloy (see Sitepu [6] and Fig. 1 for details) used in the present study has a diameter of 8 mm and 30 mm height. The details of the alloy preparation and heat treatment were described by Hara *et al.* [1,2]. SRD experiments were performed on this alloy at the ESRF ID31 in Grenoble, France, and all experimental details and the diffraction patterns obtained are given in [6,7]. ND data were measured at the high flux neutron source of the ILL Neutrons for Science in Grenoble, France, using the D1A 25-detector high-resolution neutron powder diffractometer at a wavelength of 1.9114(1) Å, from 2θ of 5° to 165° with a step size of 0.05°. During the ND data collection the D1A instrument was equipped with a cryofurnace to heat and cool the alloy (with a temperature constant zone exceeding the length of the rod alloy). After mounting the alloy in the D1A diffractometer it was heated up to (386 ± 7) K. Then, the temperature was held for 360 s to reach the thermal equilibrium and the data were measured for 6 hours. The temperature was then slowly cooled down to (290 ± 7) K and also held for 360 s to reach the thermal equilibrium. Then, the data were measured at a temperature of (290 ± 7) K for 6 hours. After that, the temperature was slowly cooled down to (250 ± 7) K where it was also held for 360 s. At this temperature, the data were measured for 6 hours. The neutron high resolution powder diffraction data from the 25-detectors were then processed to yield a single histogram using interpolations between adjacent observations to correct for zero-point offsets and detector sensitivities. As expected, the shape memory effect is based on martensitic phase transformations from the parent B2 cubic to the trigonal R-phase martensite and then to the monoclinic (B19′) martensite. The ND data sets of the phases are consistent with the differential scanning calorimetry, on cooling curve. Like the SRD data [6,7], there was no change in the appearance of the ND data when the experiment was repeated. Note that, only the R-phase ND data are reported in this paper due to the limitations of space.

Rietveld refinement results and Discussions

Unlike Sitepu [6], in this study the crystal structure refinement of the R-phase was started from the cubic parent phase with $Pm\bar{3}m$ space group ($a_c = 3.0108$ Å) and then distorted to rhombohedral $R\bar{3}m$ where the hexagonal unit cell has $a_h = a_c\sqrt{2}$ and $c_h = a_c\sqrt{3}$ and the atom positions are fixed by symmetry as Ti (0,0,0) and Ni (1/2,1/2,1/2). Removing the R-centre from this model gives space group $P\bar{3}m1$ (No. 164) and generates extra reflections which index the weaker superstructure peaks, but still miss most of the stronger extra reflections. In space group $P\bar{3}m1$ the atomic positions split into two sets with the introduction of two adjustable parameters (displacements along z for the two atoms giving the violation of the R-centre). In order to index the rest of the reflections an increase of the a axis to $a = a_h\sqrt{3}$ is required, which corresponds to a change of basis in the ab plane of the hexagonal unit cell. The corresponding maximal subgroup is $P\bar{3}1m$ (No.162) where there are now two Ni and two Ti atoms in the asymmetric unit with four adjustable parameters representing displacements along y and z. With this lattice all of the peak positions can be accounted for.

Refinement of models with symmetry $P\bar{3}1m$ did not give a good reproduction of the observed intensities and when isotropic temperatures factors were refined they tended to reach physically unreasonable values. The best model found for $P\bar{3}1m$ had $R_{WP} = 14\%$ and increasing the number of coefficients to describe the texture did not significantly improve the fit. A further reduction in symmetry was proposed with subgroups $P\bar{3}$ (No. 147), $P312$ (No. 149) and $P31m$ (No. 157) being produced when symmetry elements are removed from the $P\bar{3}1m$ model.

Combined refinements using both the ND and SRD data sets together were carried out using these space groups, giving a final series of models for comparison ($P\bar{3}1m$, $P\bar{3}$, $P312$, $P31m$ and $P3$). Removal of the two fold axis has the most dramatic impact on the fit, with all three of the models $P\bar{3}$, $P31m$ and $P3$ having similar *goodness-of-fit* indices (χ^2) with $P312$ and the parent $P\bar{3}1m$ giving rather poor fits, therefore we report the refined models from all three of the candidate space groups in Table 1. For all three of these models the agreement between observed and calculated curves is excellent, although only the refinement in space group $P\bar{3}$ converges. Large shifts on the atomic positions remain after many cycles of refinement in space groups $P31m$ and $P3$, indicating that our data were not sufficient to determine these parameters. Comparing the three models shows that $P\bar{3}$ only contains 6 atom parameters, compared to 17 for $P3$ and 11 for $P31m$.

Given that the refinements would only converge using space group $P\bar{3}$ and that no significant improvement in fit is found for the other space groups, we conclude that this space group with only six degrees of freedom in the atomic positions is sufficient to describe our data. Figure 2 depicts the excellent agreement between observed and computed data when the $P\bar{3}$ model is used. The blue tick marks represent the positions of the subcell reflections which are generated by a distortion of the cubic unit cell. At low scattering angles all of the strong peaks can be accounted for by the subcell reflections, indicating that the R-phase structure is indeed a small distortion from the high temperature cubic phase. At high angles the blue peak positions miss much of the scattered intensity, showing that these data contain a great deal of information about the structural distortion.

Comparison of the fits in Figure 3 where neutron and synchrotron data are both plotted with the same x-axis (d-spacing) shows that the peak intensities are quite different in the two data sets. This is due to the negative scattering length for Ti, so that by exploiting combined neutron and X-ray refinements there is excellent discrepancy between the two atomic sites. Trial refinements initially using only the synchrotron data sometimes found a false minimum with somewhat worse *goodness-of-fit* indices, however, when both data sets were used the same minimum was always recovered.

Figure 4 shows the pattern of atomic displacements, where the high symmetry positions are also marked by white lines in order to make the atomic displacements more clear. The displacements in space group $P\bar{3}$ were actually smaller than those found for the other models, as judged from the interatomic distances. The principal shift is of Ni6 and the change in structure can be described approximately as a buckling of the atomic planes.

Summary

The combined synchrotron and neutron structural fit shows that the reasonable space group for R-phase is $P\bar{3}$ as the six refined atomic positions were converging and the crystallographic R_{WP} and $R(F^2)$ figures-of-merits are 7.59 and 7.32% for synchrotron and 10.87 and 9.65% for neutron. The corresponding R_{WP} and $R(F^2)$ values reported by Hara *et al.* [1,2] with 17 refined positional parameters were 8.47 and 23.83% for XRD data. Their $R(F^2)$ value is twice higher than that of the corresponding value for combined synchrotron and neutron fits clearly shows that the texture should be taken care in order to get accurate results. Therefore, it can be concluded that the combined synchrotron and neutron structural refinement provides accurate crystal structure parameters for R-phase in the $P\bar{3}$ model when applying correction to intensities using the GSH description.

Acknowledgements

Thanks to Dr F. Fauth for his help in conducting the experiment. The authors wish to acknowledge Dr Alan W. Hewat of ILL for his help in conducting the early refinement with the center symmetry of the R-phase. Thanks to ESRF and ILL for providing the beam time on the project.

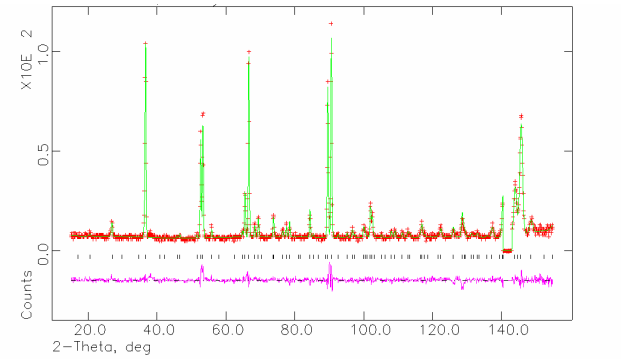

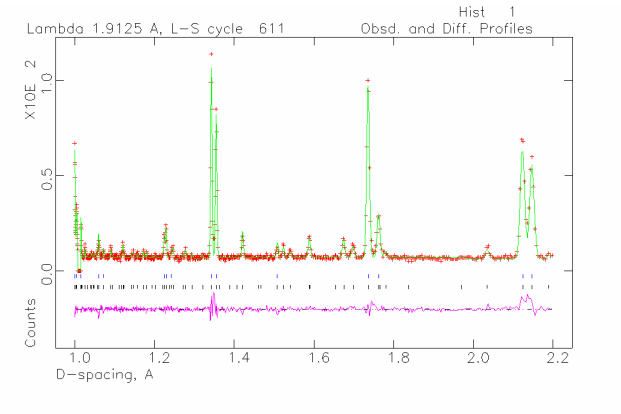

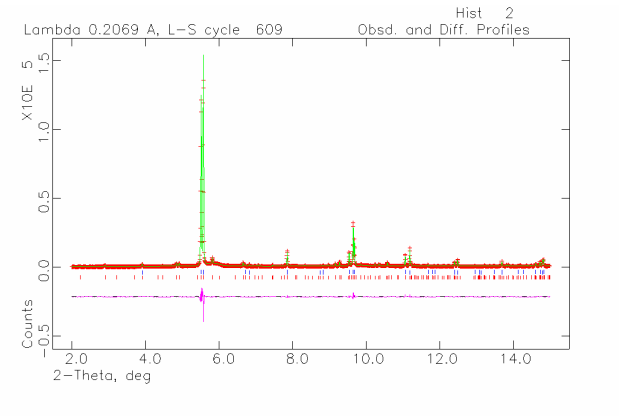

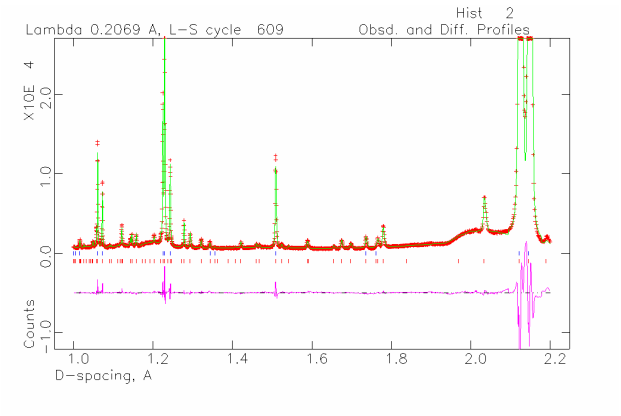

Fig. 2. The agreement between the measured and calculated neutron (top) and synchrotron (bottom) diffraction patterns for R-phase collected at 290K, on cooling, following combined refinement with the GSH description for texture.

Fig. 3. Comparison of fits to neutron (top) and synchrotron X-ray (bottom) profiles (the synchrotron X-ray data only show the lower 1/6 of the y-range, so that the weak peaks are visible).

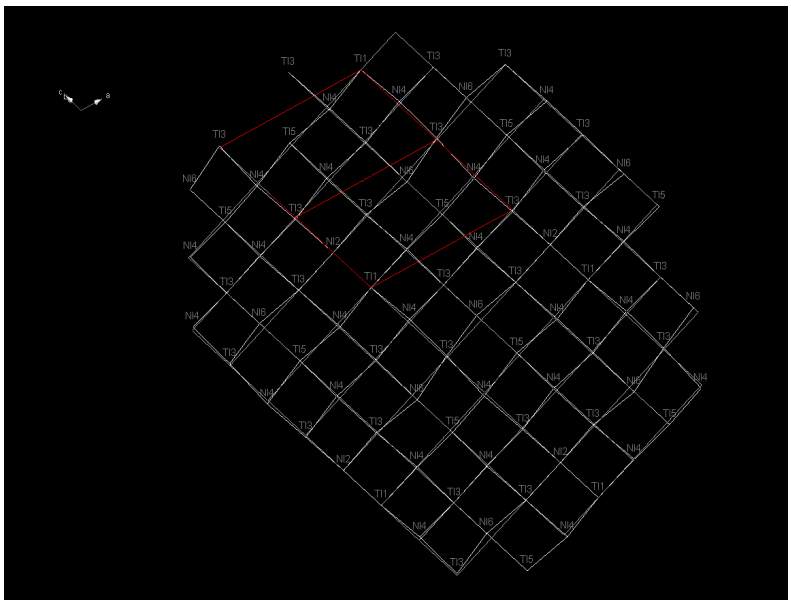

Fig. 4. The trigonal R-phase structure.

Table 1. Summary of combined synchrotron (X) and neutron (N) Rietveld 'fit' results for the models

(a) $P\bar{3}$ [R_{WP} (N)= 10.87, R_{WP} (X)= 7.59, χ^2 =5.867, $R(F^2)$ N=9.65, $R(F^2)$ X=7.32 and sh/e=0.04]

Parameters	x	y	z	100*Uiso (Å)^2	Multiplicity	Fraction
TI1	0	0	0	0.768(27)	1	0.880(4)
NI2	0	0	0.5	0.519(26)	1	1
TI3	-0.00805(23)	0.3259(5)	0.65701(27)	0.768(27)	6	0.880(4)
NI4	-0.01929(18)	0.3245(4)	0.14673(24)	0.519(26)	6	1
TI5	0.333333	0.666667	0.03045(41)	0.768(27)	2	0.880(4)
NI6	0.333333	0.666667	0.56383(37)	0.519(26)	2	1

(b) $P3$ [R_{WP} (N)= 10.79, R_{WP} (X)= 7.46, χ^2 =5. 673, $R(F^2)$ N=14.99, $R(F^2)$ X=7.83 and sh/e=45]

Parameters	x	y	z	100*Uiso (Å)^2	Multiplicity	Fraction
TI1	0	0	0	0.714(21)	1	0.875(3)
NI2	0	0	0.5249(16)	0.587(18)	1	1
TI3	-0.0129(6)	0.3248(10)	0.6463(10)	0.714(21)	3	0.875(3)
NI4	-0.0116(5)	0.3364(7)	0.1306(8)	0.587(18)	3	1
TI5	0.333333	0.666667	0.0150(20)	0.714(21)	1	0.875(3)
NI6	0.333333	0.666667	0.5301(15)	0.587(18)	1	1
TI7	0.0063(8)	0.6748(8)	0.3314(13)	0.714(21)	3	0.875(3)
NI8	0.0204(6)	0.6834(6)	0.8336(11)	0.587(18)	3	1
TI9	0.666667	0.333333	-0.0447(11)	0.714(21)	1	0.875(3)
NI10	0.666667	0.333333	0.4172(11)	0.587(18)	1	1

*Note: * Atoms 7 to 10 are generated from atoms 3 to 6 of P-3 by the inversion operation (-x,-y,-z).*
*** Atom 2 is allowed to move along z compared to model $P\bar{3}$.*

(c) $P31m$ [R_{WP} (N)= 10.88, R_{WP} (X)= 7.46, χ^2 =5. 677, $R(F^2)$ N=10.9, $R(F^2)$ X=6.27 and sh/e=26]

Parameters	x	y	z	100*Uiso (Å)^2	Multiplicity	Fraction
TI1	0	0	0	2.385(24)	1	0.876(3)
NI2	0	0	0.4714(14)	0.941(22)	1	1
TI3	0	0.3233(6)	0.6970(11)	0.709(24)	3	0.876(3)
NI4	0	0.32134(41)	0.1825(9)	0.374(22)	3	1
TI5	0.33333	0.66667	0.0579(8)	0.420(24)	2	0.876(3)
NI6	0.33333	0.66667	0.5810(12)	0.737(22)	2	1
TI7	0	0.6621(4)	0.3788(14)	0.764(24)	3	0.876(3)
NI8	0	0.64515(30)	0.8852(12)	0.494(22)	3	1

*Note: * Atoms 7 and 8 are generated from atoms 3 and 4 of model $P\bar{3}$ by the inversion and x co-ordinates are fixed by the mirror plane compared to $P\bar{3}$.*

References

[1] T. Hara, T. Ohba, E. Okunishi and K. Otsuka: Mater. Trans. JIM Vol. 38 (1997), p. 11

[2] T. Hara, T. Ohba and K. Otsuka: J. de Physique III Vol. 5 (1995), p. 641

[3] H. Sitepu, W.W. Schmahl, J. Khalil Allafi, G. Eggeler, A. Dlouhy, D.M. Többens and M. Tovar: Scripta Mater. Vol. 46 (2002), p. 543

[4] E. Goo and R. Sinclair: Acta Metall. Vol. 33 (1985), p. 1717

[5] D. Schryvers and P.L. Potapov: *Materials Trans.* Vol. 43 No. 5 (2002), p. 774

[6] H. Sitepu: Texture and Microstruc. Vol. 35 (2003), p. 185

[7] H. Sitepu, H.G. Brokmeier, D. Chateigner and J.P. Wright: Solid State Phen. (2005), In Print

[8] H. Sitepu, B.H. O'Connor and D.Y. Li: J. Appl. Cryst. Vol. 38 (2005), p. 158

[9] S. Matthies, L. Lutterotti and H.-R. Wenk: J. Appl. Cryst. Vol. 30 (1997), p. 31